AD NUMBER

AD236370

NEW LIMITATION CHANGE

TO

Approved for public release, distribution unlimited

FROM

Distribution authorized to U.S. Gov't. agencies and their contractors; Administrative/Operational Use; 30 SEP 1959. Other requests shall be referred to Air Force Cambridge Research Labs., Hanscom AFB, MA.

AUTHORITY

AFCRL ltr, 3 Nov 1971

UNCLASSIFIED

AD 236 370

Reproduced

by the

Armed Services Technical Information Agency

ARLINGTON HALL STATION; ARLINGTON 12 VIRGINIA

UNCLASSIFIED

10

THE INFLUENCE OF TERRAIN AND THERMAL STRATIFICATION ON FLOW IN THE SURFACE AND PLANETARY BOUNDARY LAYERS

BY

JAMES G. EDINGER

AND

SHIH-KUNG KAO

Department of Meteorology
University of California, Los Angeles

Final Report under Contract No. AF 19(604)-2424
30 September 1959

The research reported in this document has been sponsored by the Geophysics Research Directorate of the Air Force Cambridge Research Center, Air Research and Development Command.

THE INFLUENCE OF TERRAIN AND THERMAL STRATIFICATION ON FLOW IN THE SURFACE AND PLANETARY BOUNDARY LAYERS

BY

JAMES G. EDINGER

AND

SHIH-KUNG KAO

Department of Meteorology
University of California, Los Angeles

Final Report under Contract No. AF 19(604)-2424
30 September 1959

The research reported in this document has been sponsored by the Geophysics Research Directorate of the Air Force Cambridge Research Center, Air Research and Development Command.

TABLE OF CONTENTS

ILLUSTRATIONS

INTRODUCTION

This report presents the results of a study of the effects of terrain and thermal stratification upon the flow in the surface boundary layer and the planetary boundary layer of the atmosphere. The investigations carried out were both empirical and theoretical, the observational material consisting of the winds observed in the lowest 5 km of the atmosphere over Santa Monica, California. Here a persistent strong temperature inversion exists many days of the year between approximately 500 and 1000 m, with superadiabatic lapse rates below (daytime) and subadiabatic lapse rates above. The surrounding terrain includes a bay shaped coastline (partly mountainous and partly plain), the coastal plains and valleys backed up by moutain ranges 2 to 3 km in height.

The report consists of three parts. In Part I the Santa Monica rawin data is analysed and the features of the mean flow and the diurnal fluctuations about it are related to the inversion and the terrain features. The character of the basic flow below, within and above the inversion is described and discussed. The nature of the diurnal fluctuations about this mean flow is scrutinized in detail. It is decomposed into two oscillations possessing different orientations in the horizontal, different distributions in the vertical and different phases in both the time and vertical coordinates. Both oscillations are associated with a major terrain feature and the influence of each feature is seen to be related to the position of the temperature inverson.

Part II of the report consists of a theoretical analysis of the effects of an inversion layer and a sea-breeze on the stationary flow in a planetary boundary layer. It is shown that an intense temperature inversion virtually acts as a boundary surface which divides a planetary boundary layer into two layers. In the lower layer the flow primarily is thermally driven whereas in the upper layer the flow is similar to that in a boundary layer of a homogeneous fluid. The inversion layer moves in the direction of the resultant of the stresses acting on the layer by the fluids above and below it. A theoretical model is constructed and checked against the observed flow at Santa Monica.

Part III presents a theoretical discussion of the very lowest layer of the atmosphere, the surface boundary layer, and its response to different thermal stratifications. An analysis is made of some characteristics of the steady turbulent transfer in the boundary layer of a stratified fluid. The effect of the heat flux on the variation of the mixing length and the flux Richardson number with height is determined. The velocity and temperature profiles are derived. It is found that for a constant free stream velocity an upward heat flux increases the friction velocity, whereas a downward heat flux decreases the friction velocity. The lower limiting value of the flux Richardson number is found to be -0.5, which together with the upper limiting value, 0.5, obtained by Townsend, gives the range of the flux Richardson number. Velocity profiles for the non-neutral conditions converge in the higher level towards the profile for the neutral condition, a characteristic which agrees with the classical velocity profiles observed by Thornthwaite and Kaser.

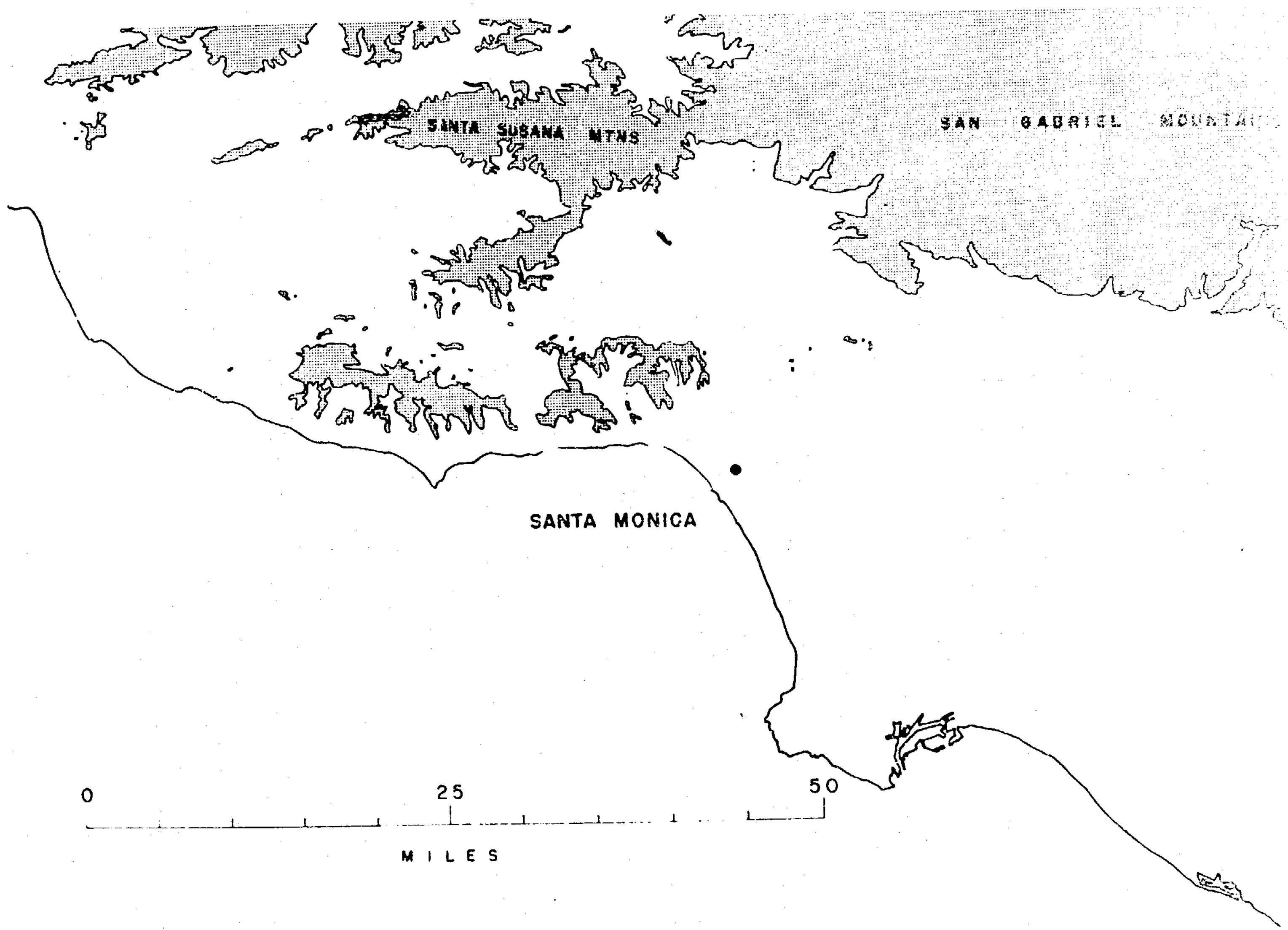

Figure 1-1 Map of Los Angeles area, (shaded area – land above 1500' msl)

PART I

WIND STRUCTURE IN THE LOWEST 5 KM ABOVE SANTA MONICA, CALIFORNIA

by James G. Edinger

1. Introduction

This section describes and analyses the summertime wind structure in the lowest 5 km of the atmosphere above Santa Monica, California and attempts to determine the influence of complex orography and a persistent inversion on the flow across the coastline.

2. Geography

The geometry of the Santa Monica area deviates in several repects from a flat plain with a straight coastline. As seen in figure 1-1 the coastline is bay shaped consisting of an east-west shoreline at the base of the Santa Monica Mountains and a north-northwest south-southeast oriented shoreline at the western terminus of the Los Angeles coastal plain. The dominating orographic feature inland is a complex of mountain ranges about 25 miles north of Santa Monica oriented roughly east-west and rising on the average to 2 km, some peaks exceeding 3 km. Beyond these ranges lie the high deserts and the southern end of the San Joaquin Valley.

3. Data

The data used are the checked radiosonde winds aloft reports for Santa Monica for July and August, 1957 and 1958. Chosen for study were those days on which a strong inversion was reported by the 1600 PST radiosonde and on which the wind at the 3 km level was from the 40° sector between 166° and 206.° About one out of four days met both requirements providing a sample size of 29 days. The subsequent discussion is based on resultant winds computed from this data for the surface, 150, 300, 500, 1000, 1500, 2000, 2500, 3000, 4000, and 5000 m levels for the four observation times of 0400, 1000, 1600 and 2200 PST.

Figure 1-2 gives the mean position and strength of the inversion for 1600 PST on these days. The inversion layer in the mean extended from 328 m to 820 m with an increase of temperature from the bottom to top of 8.7°C. The layer below the inversion was superadiabatic in the mean with a lapse rate almost double the dry adiabatic rate. The layer above was subadiabatic with a lapse rate about two thirds of the dry adiabatic rate.

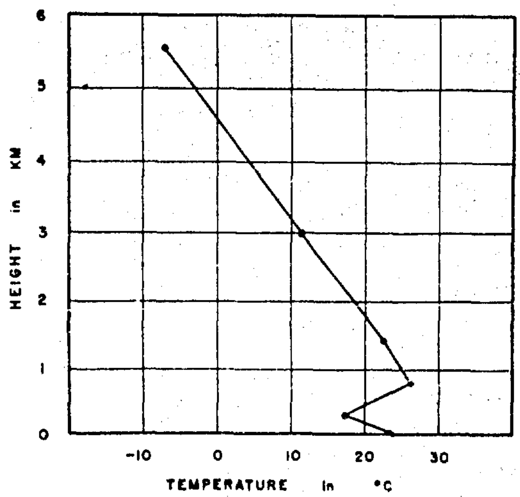

Figure 1-2
Mean temperature sounding at Santa Monica, 1600 PST

4. Basic flow

Figure 1-3 gives the height* hodograph of the resultant winds obtained when data from all four observations times, 0400, 1000, 1600 and 2200 PST, are combined to provide a representation of the basic flow.

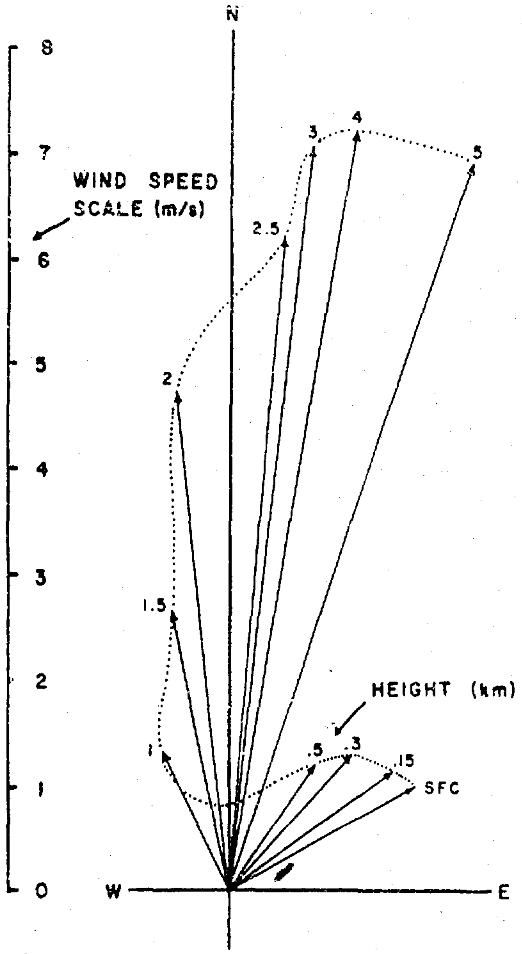

Figure 1-3
Height hodograph averaged for all observation times, Santa Monica

Below the inversion, in the layer from the surface up to 300 m, the wind is directed inland approximately normal to the Santa Monica coastline at about 2 m/sec, the result of a strong daytime sea-breeze added to a weak nighttime land-breeze. Above the inversion the wind velocity increases systematically from 1.5 m/sec at 1000 m to 7.5 m/sec at 5000 m from the southerly quadrant and turns progressively to the right with increasing height. The southerly direction of the flow at these levels compares favorably with the direction of the geostrophic wind as given on the 700 mb charts for these 29 days. On most of these maps a north-south trough is indicated west of the Southern California coast separating the sub-tropical high in the Eastern Pacific Ocean from a high pressure system over the continent.

The wind velocity in the inversion layer, 300 m to 1000 m. has little change in magnitude from bottom to top but its direction changes by almost 70° indicating that this extremely stable layer is the region of marked directional shear between lower west-southwesterly and upper southerly wind regimes.

5. Diurnal fluctuations

Figure 1-4 presents the diurnal variations of the velocity about this basic flow in the form of time hodographs for each level from the surface up to the 5 km level. Each hodograph consists of the four vectors representing the velocity relative to the basic flow at 0400, 1000, 1600 and 2200 PST. These four vectors are plotted at the end point of the velocity vector of the basic flow so that the relative orientation and magnitude of the fluctuation and the basic flow are apparent.

* Two types of hodographs will be discussed: (a) one showing the variation of velocity with height and (b) one showing the variation of velocity with time of day. To distinguish the two the modifiers "height" or "time" will be used.

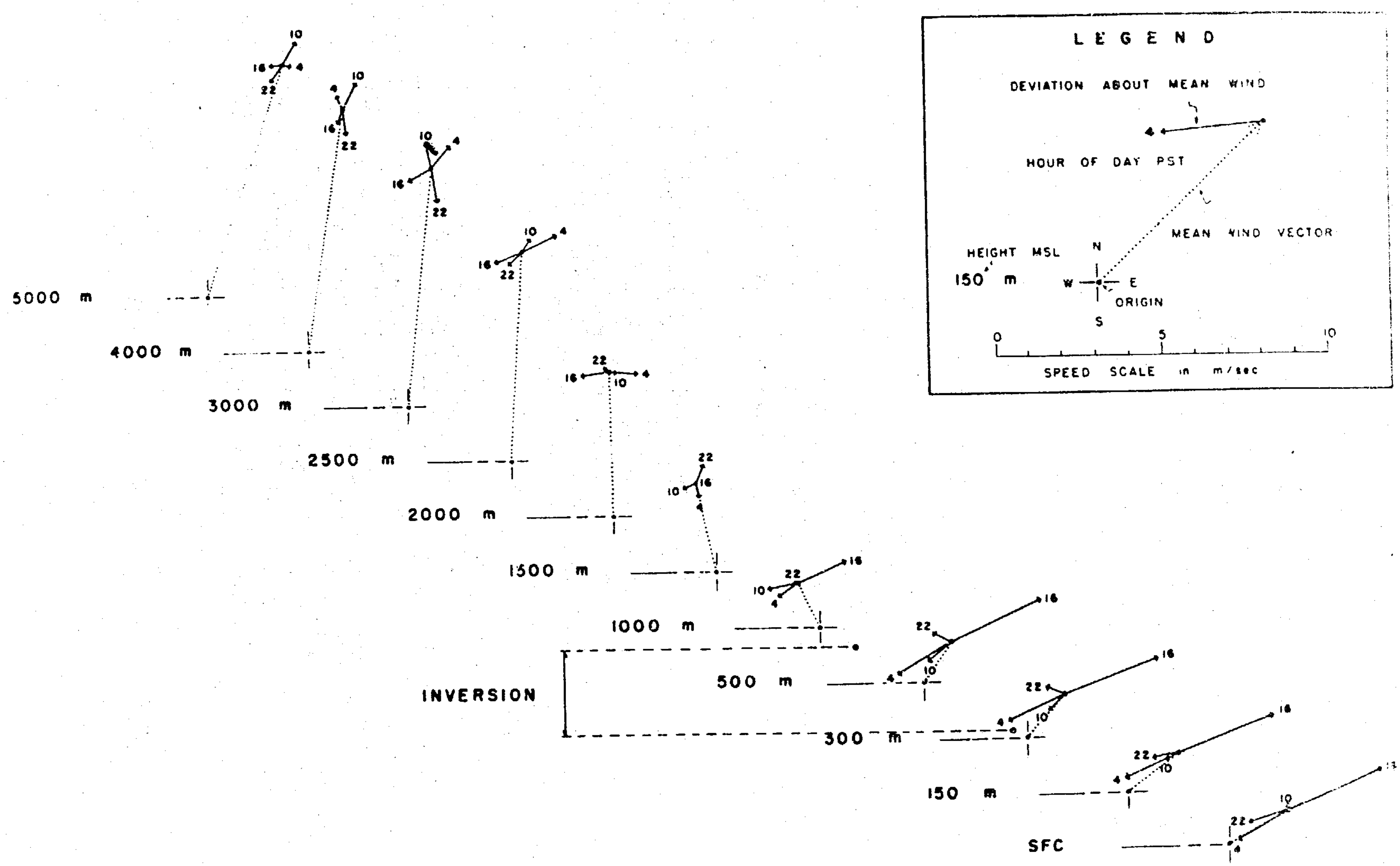

Figure 1-4 Time hodographs for all levels, surface to 5 km, Santa Monica

The inversion layer is seen to be the seat of marked changes not only in the basic flow but in the character of the diurnal oscillation as well. Whereas the mean flow, as mentioned above, changes direction abruptly here, the magnitude of the diurnal oscillation suffers an abrupt dimunition in magnitude.

In the lowest 500 m the diurnal oscillation of wind velocity is largest, about 5 m/sec in magnitude along the 60°–240° axis with maximum on-shore (240°) component at about 1600 PST. Above 500 m the magnitude of the 60°–240° oscillation decreases rapidly reaching zero at 1500 m. Above 1500 m its phase is reversed (maximum on-shore component at 0400 PST) and its manitude increases to a new maximum of 2 m/sec at 2500 m. Above 2500 m the magnitude of the oscillation decreases to about 0.5 m/sec at 4000 and 5000 m, the phase remaining unchanged.

This oscillation in the 60°–240° vertical plane has the characteristics generally ascribed to a sea-land breeze regime. However, the observed fluctuations in velocity are not confined entirely to the 60°–240° vertical plane. Components of motion outside this plane become more pronounced as height increases. At the 3, 4 and 5 km levels the maximum oscillation is more nearly along the 180°–360° axis than the 60°–240°. Furthermore, the oscillation in this north-south plane apparently has a phase that lags about 6 hours behind the 60°–240° oscillation. Figure 1-5 contrasts the observed changes in velocity from 0400 to 1600 PST with those from 1000 to 2200 PST at all levels. Whereas the velocity variations with the 0400 to 1600 PST phase are seen to be confined mostly to the 60°–240° direction, those with the 1000 to 2200 PST phase appear to be more nearly oriented along a 180°–360° axis.

The observed velocity fluctuations, then, are better described as a superposition of two oscillations than by only one. Figure 1-6 provides the observed magnitudes of the 60°–240° and 180°–360° oscillations as a function of height. There are several obvious differences between the two distributions: (1) The strength of the lower branch of the 60°–240° oscillation is much greater than that of the lower branch of the 180°–360° oscillation, the upper branches of both being of about the same strength, and (2) The level separting the upper and lower branches of the two oscillations are displaced 500 m with respect to each other, the 180°–360° oscillation reversing at about 2000 m, the 60°–240° at 1500 m.

If the two oscillations were in phase timewise, the resultant hodographs would be simple lines, enclosing no area. Since, however, there is a time lag between the two, the hodographs open out into closed curves. Furthermore, the displacement in the vertical of the two oscillatory pattern with respect to each other determines the sense of rotation of the vectors in the time hodographs. If both patterns reversed their direction of flow at the same height, the sense of rotation would be the same at all levels. Since, however, the reversal takes place at 1500 m for the 60°–240° oscillation and at about 2000 m for the 180°–360°, the sense of rotation is reversed between these two levels.

Figure 1-7 shows what the time hodograph would be for each level if the vector sum of these two oscillations, 6 hours out of phase timewise and 500 m out of phase heightwise, completely described the motion. For comparison purposes it also displays the corresponding observed time hodographs.

There is general agreement between the synthesized and observed time hodographs. Even the sense of rotation of the vectors is correctly described at almost all levels, the predominant counterclockwise rotation giving way to clockwise only in the vicinity of the 1500-2000 m

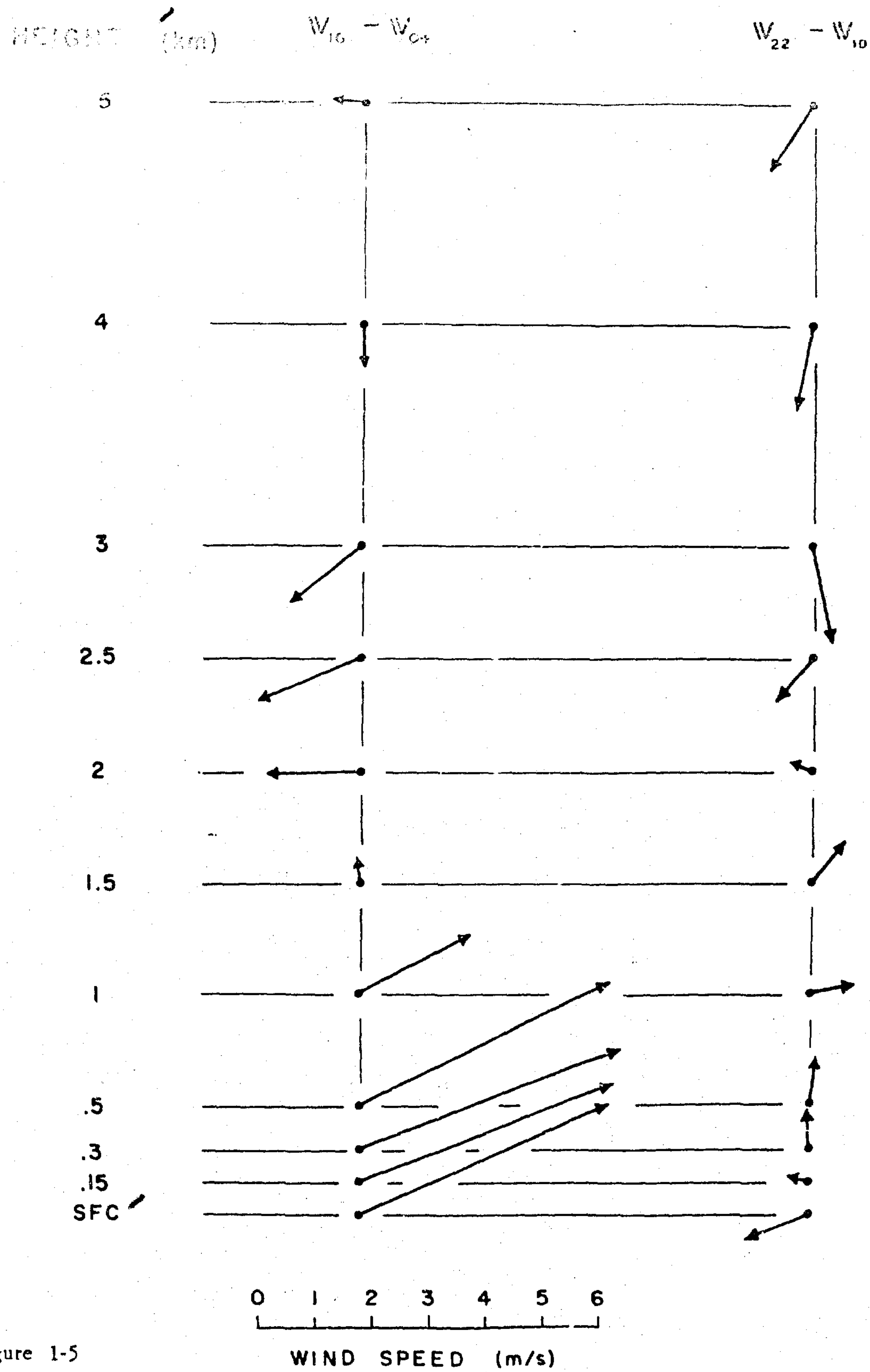

Figure 1-5

Velocity changes, 0400 to 1600 PST, versus velocity changes, 1000 to 2200 PST

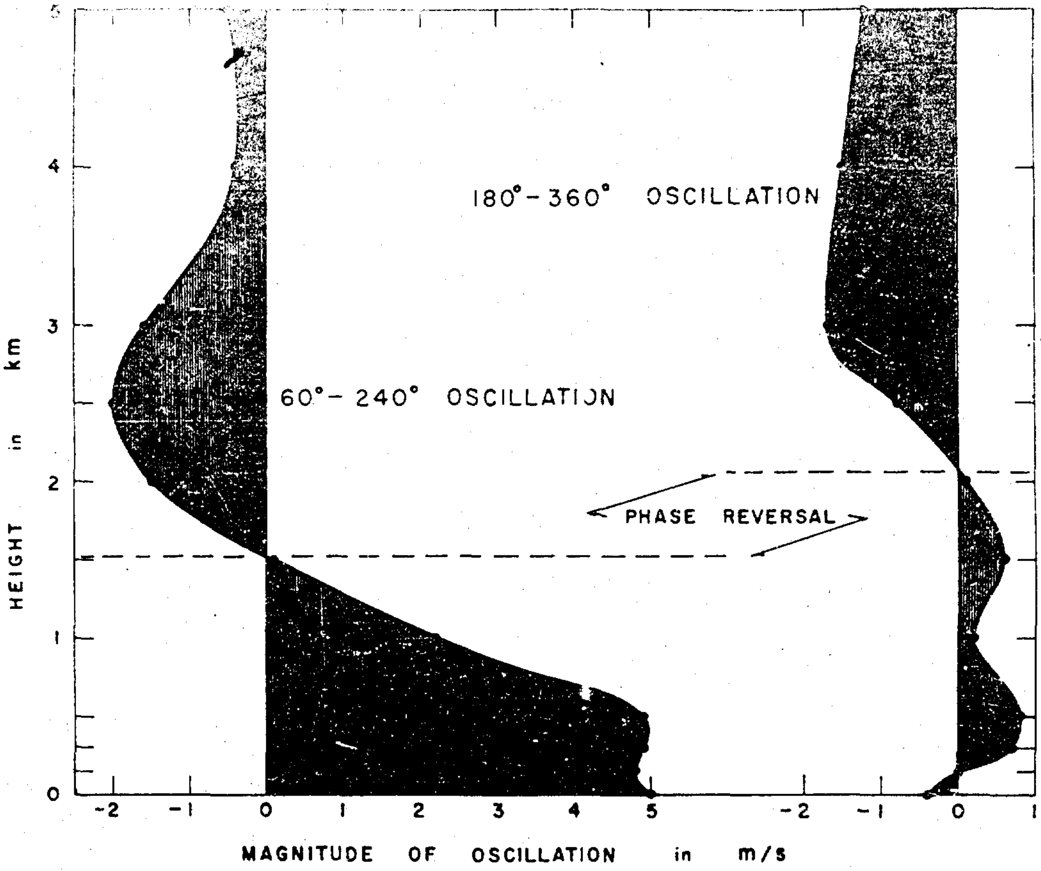

Figure 1-6 Magnitudes of the 60°–240° and 180°–360° oscillations as a function of height

layer where a 180° shift in the relative phase of the two oscillations results from their 500 m relative displacement in the vertical.

To reveal more completely the details of the motion in the 60°–240° and 180°–360° vertical planes, time sections for both are presented in figures 1-8 and 1-9. The obvious tilt of the systems toward increasing time with increasing height indicates that the phase of neither oscillation is actually constant with height. Oscillations at higher levels consistently lag behind those below. Similar behavior was observed in the Batavia sea-breeze by van Bemmelen,(1) (1922), see figure 1-10. The upper branch of the circulation over Batavia reaches its maximum speed about 1.5 hours after the maximum occurs in the lower branch. For Santa Monica this lag is 2.5 hours for the 60°–240° circulation and 3.5 hours for the 180°–360° circulation. The lag between the 60°–240° and 180°–360° circulations at Santa Monica is seen to be closer to 3 hours than to 6 hours as suggested by the simplified analysis above.

The general dimensions of the diurnal circulation above Batavia and Santa Monica are about the same. The maximum return flow aloft occurs at 2 km in the former and at 3 km in the latter. Although Santa Monica's circulation is deeper it is only about half as strong.

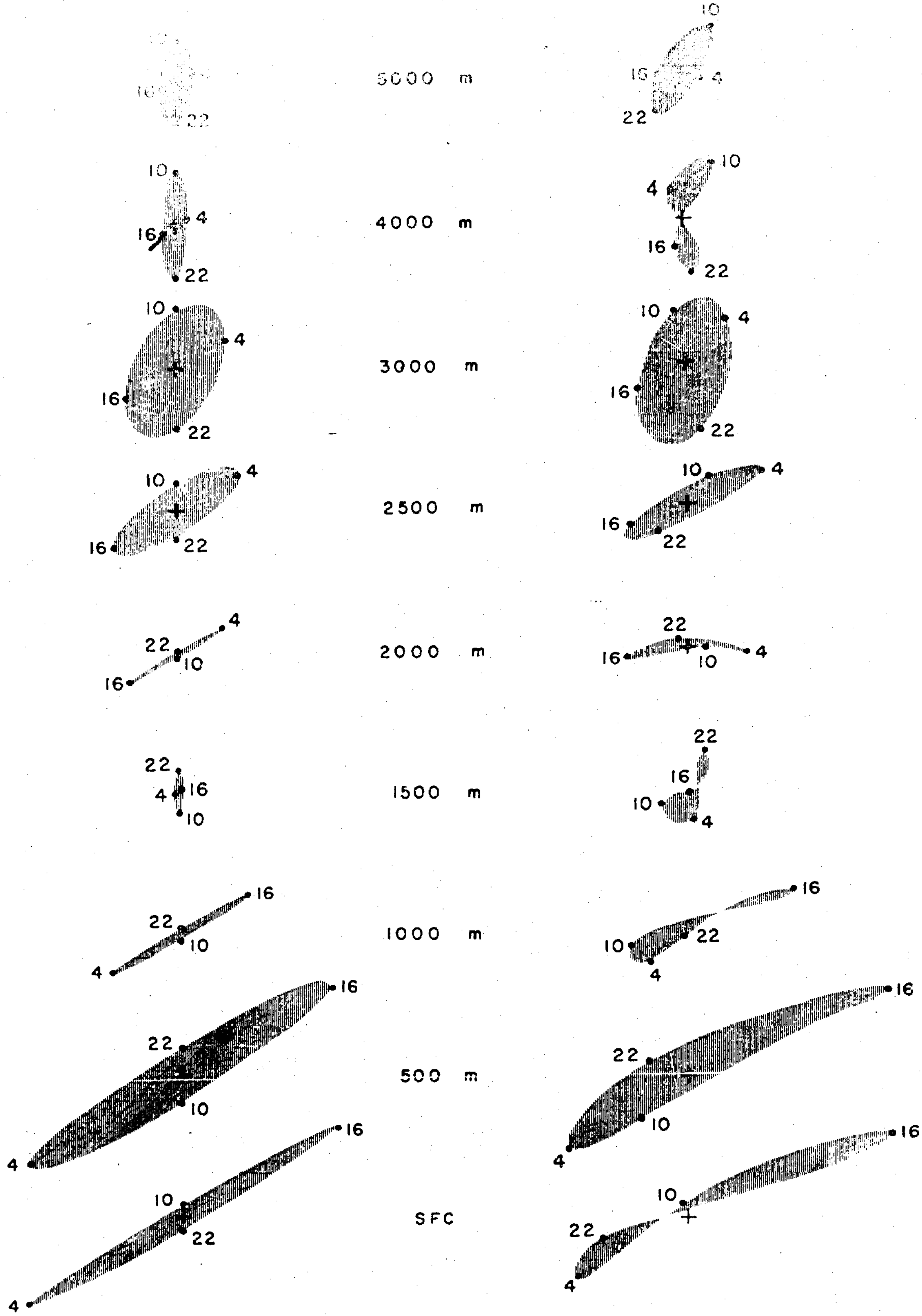

Figure 1-7 Synthesized time hodographs (left) versus observed time hodographs (right)

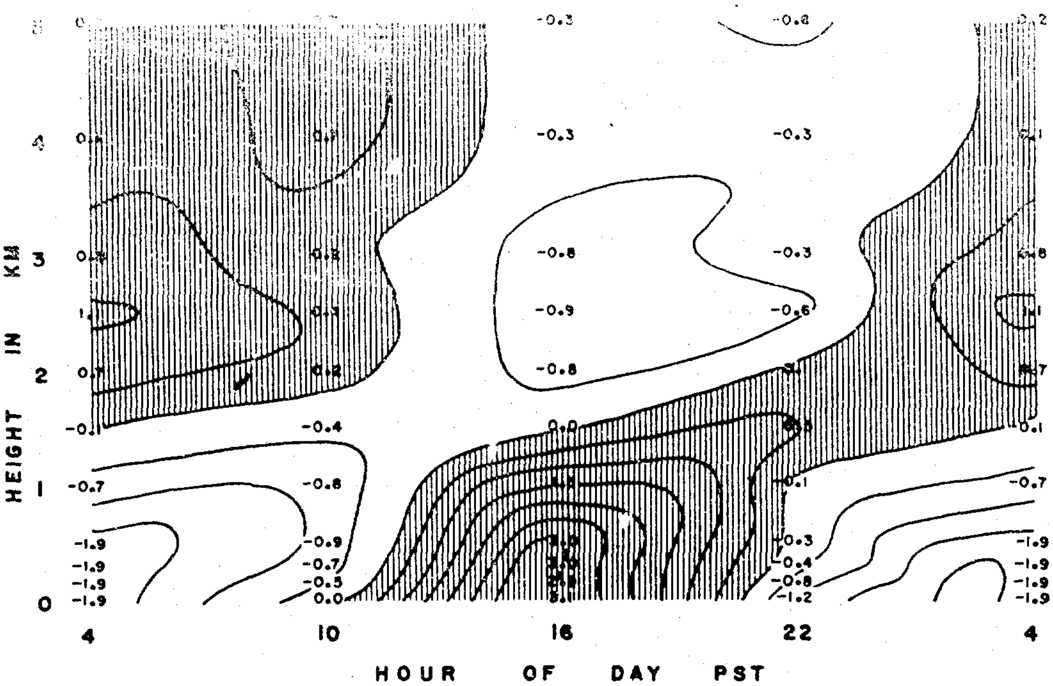

Figure 1-8 Time section in the 60°–240° vertical plane, Santa Monica (speed in m/sec)

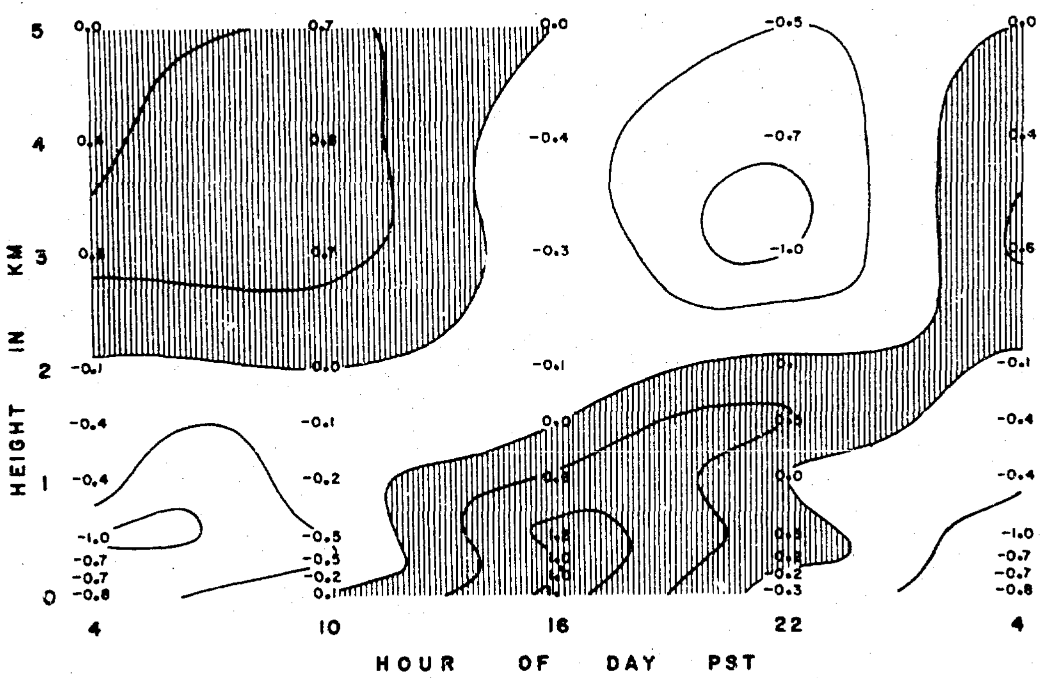

Figure 1-9 Time section in the 180°–360° vertical plane, Santa Monica (speed in m/sec)

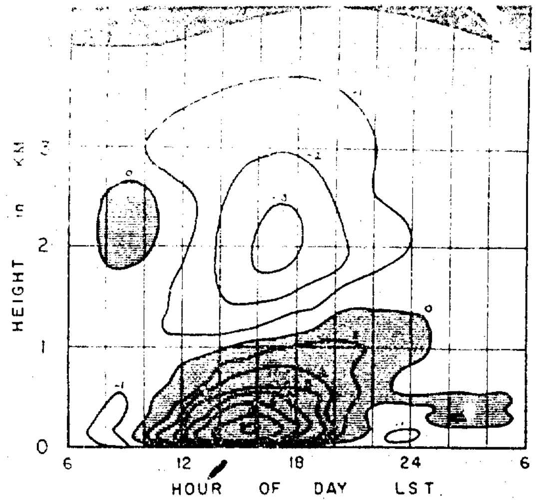

Figure 1-10

Time section of Batavia sea-breeze in vertical plane normal to coast. (speed in m/sec)

Batavia's upper and lower flows have maximum speeds of 3 and 7 m/sec respectively contrasted with 1 and 3 m/sec for Santa Monica. At both cities the maximum depth of the circulation is reached in late afternoon. As interesting point of difference is revealed by considering the heights of occurence of the maximum sea-breeze: at Santa Monica it is found at the surface and at Batavia at about 150 m above the surface. However, it is likely that the speed of Santa Monica's surface sea-breeze is exaggerated because the observation is taken at the top of a bluff that faces directly into the sea-breeze. Pilot balloon observations taken at U.C.L.A., a few miles inland, indicate a maximum well above the surface as shown in figure 1-11, the data indicating the flow beneath the inversion to be a modified channel flow with a maximum speed a little below the middle of the layer, not at the ground.

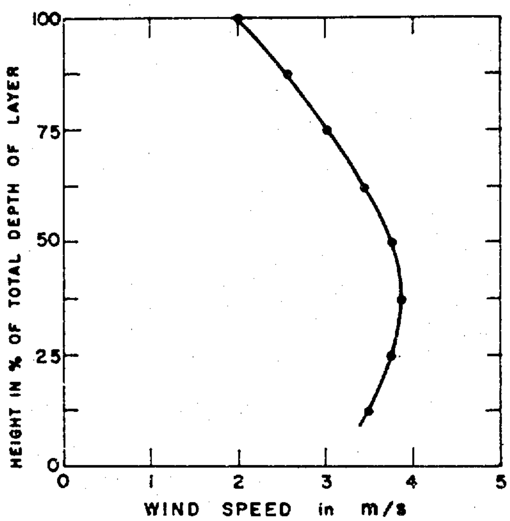

Figure 1-11

Speed of sea-breeze versus height in marine layer, U.C.L.A.

6. Interpretation

The foregoing description of the flow across the coastline at Santa Monica has several unique features that distinguish it from observed patterns at other coastline locations as well as from patterns prescribed by the various sea-breeze theories. The attempt is made here to relate these distinguishing features to geographic and atmospheric configurations peculiar to the Santa Monica area.

The mean flow (diurnal variations averaged out) has a unique structure apparently related to the persistent and strong inversion above Santa Monica. Below the inversion a monsoon flow exists, on-shore parrallel to the Santa Monica mountains. Its profile resembles channel flow but its direction shifts gradually toward the direction of the flow above it. In the inversion layer the direction of flow changes rapidly resulting in a strong directional shear. Above the inversion the flow turns slowly to the right in a manner approximating an Ekman spiral, finally assuming the direction of the geosrophic wind at heights above 2.5 km. In the next section of this report Kao (1959) develops a theoretical model for steady flow in a layer of air bisected horizontally by a strong temperature inversion. His model reproduces the major features of this observed mean flow above Santa Monica.

Concerning the diurnal variations in the flow pattern no theoretical description has been attempted although the nature of certain relationships between terrain features and the observed atmospheric oscillations are suggested by the data and may provide fruitful topics for later theoretical investigations. The fact that the somewhat complex observed oscillatory pattern can be approximated by two superposed simple oscillations suggests that in addition to the area of strong differential heating along the coastline there must be somewhere else another area almost as effective in producing a diurnal oscillation of flow.

The oscillation along the 60°–240° axis has the characteristics of the conventional sea-land breeze at a coastline. However, the coastline is strongly curved in the vicinity of Santa Monica. Consequently, it is not clear just what orientation the sea-land breeze regime should take. The fact that it moves almost perpendicular to the shoreline in the immediate vicinity of Santa Monica may in large part be the result of the roughly east-west steering action of the Santa Monica Mountains several miles to the north. The relatively dense 500 m thick layer of cool marine air lying beneath the strong persistent inversion provides a very stable configuration. The Santa Monica mountains, somewhat higher than 500 m on the average, therefore, constitute an effective constraint on the direction of flow of this layer.

The oscillation along the 180°–360° axis, on the other hand, lags 3 hours behind the 60°–240° oscillation and might be the result of differential heating along an east-west line at some distance from Santa Monica and at a height above the steering influences of the Santa Monica mountains. Such heating is likely along a different sort of "coastline" some 20 miles north of Santa Monica, the line of demarkation that lies between the top of the marine layer and the mountain ranges that rise above it. The shaded area in figure 1-1 represents the land that stands above this "ocean" of marine air, i.e. the terrain above the 1500 ft contour. It has, roughly speaking, an east-west orientation. Of course, even in the absence of the marine layer and the strong inversion differential heating would take place here between the air in contact with the mountains and that at the same level but above the coastal plain. The inversion, however, by preventing the convective transfer of heat to the air layers above the marine layer intensifies and localizes the differential heating along a zone at about 500 m elevation along the southern slopes of the mountain ranges. Interesting corroborative evidence may be the observed fact that the 180°–360° oscillation is displaced vertically about 500 m with respect to the 60°–240° oscillation.

If this upper "coastline," 20 miles inland of the regular coastline, is the seat of the 180°–360° oscillation, the effect of the differential heating must be propogated southward at a rate of 3.5 m/sec relative to the ground, 6.5 m/sec relative to the air (3 m/sec headwind) in order to arrive over Santa Monica with the observed phase lag of 3 hours. This rate of propogation is similar to that obtained from the Batavia data. There a mountain range parallels the coast some 50 to 75 km inland. The phase lag at the 500 m level (about 50 km from the coast) is about 1.5 hours. Assuming no mean wind, the monsoon roughly parallel to the mountains, the rate of propogation would be 10 m/sec. It appears that at both Batavia and Santa Monica the phase lag with height could be ascribed to effects originating on the distant mountain slopes.

Just as the Santa Monica mountains steer the low level fluctuations, the inland mountain ranges apparently block them. This is evident in the 180°–360° component of the fluctuations. It was pointed out in the discussion of figure 1-6 that the lower branch of the 180°–360° oscillation was much weaker than the upper branch. It is significant that the depth of the lower branch just about matches the average height of the mountain range, approximately 2 km. Fluctuations at the mountain slopes are constrained to move up and down the slopes producing a vertical fluctuation. This vertical fluctuation must have maximum amplitude near the ridge top and decrease with increasing height above, producing a fluctuating convergence of the vertical component there. Such a fluctuating convergence pattern would be reflected in an increase in

the magnitude of the horizontal velocity fluctuations in the upper flow, (at levels higher than the ridges). The fact that the 60°–240° oscillation at heights above 2 km is just as large as the 180°–360° oscillation yet receives no amplification due to mountain slopes is one of the several indications that this oscillation is the more vigorous of the two. It seems likely that the proximity of Santa Monica to the coast and remoteness from the inland mountain ranges would prescribe that the 60°–240° oscillation be the dominant component.

One component prescribed by the sea-breeze theories undetectable in the observations is that due to the coriolis acceleration. Theory based on flat terrain and a long straight coastline requires the time hodographs to have a clockwise rotation. At Santa Monica they are observed to have the opposite rotation almost exclusively, the major exception being in the layer between 1500 and 2000 m where the effect of the lower branch of the fluctuation set up by the inland mountain ranges combines with the upper branch of that originating at the coast to produce a clockwise rotation. It is apparent that the influence of the inland mountain ranges, like that of the coastline, is a first order effect in determining the nature of the diurnal flow patterns and that the coriolis effect must be regarded as of second order.

7. Conclusions

The mean flow of air over Santa Monica in summer in the presence of a southerly geostrophic wind at 700 mb can be conveniently subdivided into three layers: (1) below the inversion – monsoon, (2) in the inversion – strong directional shear and (3) above the inversion – Ekmon spiral. Superposed on this somewhat complex mean flow is a diurnal sea-land breeze oscillation consisting of a lower branch about as deep as the inland mountain ranges are high, (2000 m) with a return flow aloft of similar depth. This diurnal oscillation can be represented as the sum of two different oscillations and therefore appears to be the result of differential heating effects in two areas; (1) along the coastline of Santa Monica Bay and (2) along the "shore" of the "ocean" of marine air, at 500 m elevation along the southern slopes of the inland mountain ranges The difference in orientation, height add proximity of these two "shorelines" with respect to Santa Monica apparently prescribe the major features of the complex configuration of the sea-land breeze circulation.

The inversion influences the flow patterns by virtually prohibiting the vertical transfer of heat and momentum. It plays the role of the "ground" for the flow above 500 m above Santa Monica. This mean flow which resembles the Ekman spiral represents an elevated planetary boundary layer. The inversion plays a similar role in the thermal circulation set up at the mountain slopes, in this case, being analagous to the sea surface, the mountain slopes near the 500 m level being taken as the beach. In the case of the thermal circulation set up at the real coastline, however, it forms neither top nor bottom of the circulation. Here it constitutes a kind of insulating layer interior to the lower branch of the circulation where the magnitude of the oscillation begins to decrease rapidly with height.

The effect of the coriolis accelaration on the flow pattern is evidently overwhelmed by the much larger influences of the terrain features. The clockwise turning of the velocity vector in the time hodographs occurs only where terrain effects dictate this behavior.

These results, though suggestive, are tentative. They depend for verification or repudiation upon: (1) similar studies of observational material from areas of diverse orography and thermal stratification and (2) theoretical investigations of disturbances in the field of motion brought about by differential heating on a diurnal schedule associated with terrain features and coastlines.

REFERENCES

(1) Bemmelen, W. van, 1922: Land- und Seebrise in Batavia. <u>Beitr. Phys. freien Atmos.</u>, vol 10, nos. 2-3, pp. 169-177.

(2) Defant, F., 1950: Theorie der Land- und Seewinde. <u>Arch. Meteor. Geophys. Biokl.</u>, 2(A): 404-425.

PART II

STATIONARY FLOW IN THE PLANETARY BOUNDARY LAYER WITH AN INVERSION LAYER AND A SEA BREEZE

S.–K. Kao

1. Introduction

In recent years, synoptic analysis of the lower troposphere over the coastal plain of California shows that during the summer seasons a temperature inversion occurs in the layer between 500 and 1000 m on the average. (Neiburger, Beer and Leopold, 1944). Under this inversion layer a land-sea breeze prevails. On account of the presence of this inversion layer, the flow in the planetary boundary layer deviates greatly from that in a homogeneous fluid. A detailed description and discussion of the diurnal wind distribution at various levels over Los Angeles Basin has been given by Edinger (1959). It is the objective of this note to examine the effect of a temperature inversion and a sea-breeze on the stationary flow in the planetary boundary layer as a first step to the understanding of the mechanism of this system.

2. Quasi-stationary wind distribution in the planetary boundary layer

The presence of a sea-breeze in the lower layer of the planetary boundary layer makes it difficult to attain a stationary flow. As a first approximation to a stationary state and to bring out the effect of the sea-breeze, we use the observation taken at the time when the sea-breeze approaches its maximum. To bring out the effect of the wind at the geostrophic level we considered the winds at this level occurring in the 40° sector from 166° to 206° degrees. In so doing we obtain a sample of data of 29 cases from the rawin soundings taken during July and August, 1957 and 1958, at Santa Monica Airport, California. The average temperature, Fig. 1-2 shows an intense inversion layer occurring at a height between 328 m and 820 m. The planetary boundary layer consists, therefore, of three layers, the inversion layer, and the layers below and above it. The distribution of the average winds at various levels is represented by large dots in Fig. 2-1. Two characteristic features appear in this hodograph: (1) In the lower layer, say below 1 Km, the wind turns toward the left with height, whereas in the upper layer it turns toward the right. (2) In the lower layer the speed of the wind first increases with height, then decreases to a minimum at a height about 1 Km; in the upper layer wind speed generally increases with height.

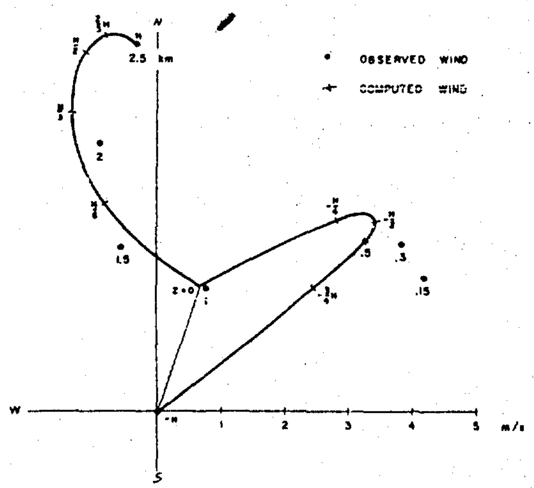

Figure 2-1
Observed versus computed winds, Santa Monica, 1600 PST

It is interesting to note that in the lower layer the hodograph bears no resemblance to the classical wind distribution in a planetary boundary layer of a homogeneous fluid (Ekman, 1902; Åkerblom, 1908; Taylor, 1916; Rossby, 1932; Rossby and Montgomery, 1935). The turning of the wind toward the left instead of right with height indicates that the Coriolis force is definitely small as compared with other forces. Furthermore, analysis of winds for

various cases shows that strong velocity shears exist between the inversion layer and its neighboring fluid. It is clear that the occurrence of these shearing stresses is due to the intense stability of the inversion layer which virtually acts as a boundary and prevents the transports of both momentum and heat from one side to the other. The flow in the lower layer therefore, is primarily governed by the sea-breeze subjected to the boundary effects of the inversion layer and at the surface of the earth. It is known both from observations and theories (Van Bemmelem, 1922; Haurwitz, 1947; Schmidt, 1947; Defant, 1950; Pierson, 1950; Pearce, 1955; Smith, 1955) that above a sea-breeze a comparatively weak land-breeze occurs. On account of the presence of an inversion layer the effect of land-breeze in the upper layer would be greatly reduced and that the flow in the upper layer is similar to that in the boundary layer of a homogeneous fluid.

3. Theoretical Model

To construct a simple model bringing out the major effects of an inversion layer and a sea-breeze on the flow in the planetary boundary layer, we idealize the inversion layer to a surface of discontinuity in temperature. On account of its extreme stability, the surface of discontinuity may be considered as a boundary surface which isolates the transfers of momentum and sensible heat from one side to the other of the surface. The planetary boundary layer consists, therefore, of two layers, one above and the other below the surface of discontinuity. In the upper layer the flow is controlled by the pressure, Coriolis and frictional forces, whereas in the lower layer we assume, for simplicity, that the flow is primarily thermally driven and that the Coriolis effect may be neglected. The equations of motion for the upper and lower layer are respectively

$$K_1 \frac{d^2}{dz^2}(u_1 + iv_1) - if(u_1 + iv_1) = \frac{1}{\rho_1}\left(\frac{\partial p_1}{\partial x} + i\frac{\partial p_1}{\partial y}\right) \equiv -if(u_g + v_g) \tag{1}$$

$$K_2 \frac{d^2}{dz^2}(u_2 + iv_2) - \frac{1}{\rho_2}\left(\frac{\partial p_2}{\partial x} + i\frac{\partial p_2}{\partial y}\right) = 0 \tag{2}$$

where K is the coefficient of eddy viscosity, ρ the density, p the pressure, $f = 2\,\Omega \sin\phi$ is the Coriolis parameter; subscripts 1 and 2 are respectively referred to the upper and lower layer, the x,y,z axes are respectively oriented toward the east, north, zenith. $V = u+iv$ and $V_g = u_g + iv_g$ are respectively the horizontal and geostrophic velocities.

Let the horizontal axes be coincided with the surface of discontinuity which is assumed to be horizontally oriented. The kinematic boundary condition requires the velocity to be continuous at the surface of discontinuity of which the velocity is denoted by $Vd = ud + ivd$. We have

$$\text{at } z = 0: \qquad u_1 = u_2 = u_d, \qquad v_1 = v_2 = v_d \tag{3}$$

Furthermore, we assume that the surface of discontinuity acted on by the air from above and below moves in the direction of the resultant of the velocity shears at this surface

$$\text{at } z = o: \quad u_d = c_o\left\{\frac{\partial u_1}{\partial z} - \frac{\partial u_2}{\partial z}\right\}, \qquad v_d = c_o\left\{\frac{\partial v_1}{\partial z} - \frac{\partial v_2}{\partial z}\right\} \tag{4}$$

where c_o is a constant.

The other boundary conditions are

$$\text{at } z=\infty : \quad u=u_g , \quad v=v_g \tag{5}$$

$$\text{at } z=-H : \quad u=v=o \tag{6}$$

where H is the height of the surface of discontinuity.

The general solution of (1) is

$$u_1+iv_1 = u_g+iv_g + c_1 e^{-(1+i)\zeta z} + c_2 e^{(1+i)\zeta z} \tag{7}$$

where $\zeta = (f/2K_1)^{1/2}$, c_1 and c_2 are two constants.

Applying the boundary condition (5) to (7), we have $C_2 = 0$. Eq. (7) becomes

$$u_1+iv_1 = u_g+iv_g+c_1 e^{-(1+i)\zeta z} \tag{8}$$

For the convenience of later discussion let H be the height at which the wind blows parallel to the isobars. We have $\zeta = \pi/H$ and, therefore $K_1 = \frac{1}{2} f (H/\pi)^2$.

If we now apply the kinematic boundary condition (3) to (8), we have

$$C_1 = \{ (u_d-u_g) + i(v_d-v_g) \} \tag{9}$$

Substitution of (9) in (8) gives

$$u_1+iv_1 = u_g+iv_g + \{(u_d-u_g) + i(v_d-v_g) \} e^{-(1+i)\zeta z} \tag{10}$$

for $z \geq 0$

For simplicity, we assume that the horizontal pressure gradient is constant in the lower layer. It can be shown that the solution of (2), which satisfies the boundary conditions (3) and (6), takes the form

$$u_2+iv_2 = \frac{1}{2\rho_2 K_2}\left(\frac{\partial p_2}{\partial x} + i\frac{\partial p_2}{\partial y}\right)\left\{\left(z+\frac{H}{2}\right)^2 - \left(\frac{H}{2}\right)^2\right\} + (u_d+iv_d)\left(1+\frac{z}{H}\right) \tag{11}$$

for $0 \geq z \geq -H$.

Let us define the sea-breeze velocity, $V_s = u_s + iv_s$, as the velocity in the lower layer if the surface of discontinuity is at rest. Putting $u_d = v_d = 0$ in (11) we have

$$u_s+iv_s = \frac{1}{2\rho_2 K_2}\left(\frac{\partial p_2}{\partial x} + i\frac{\partial p_2}{\partial y}\right)\left\{\left(z+\frac{H}{2}\right)^2 - \left(\frac{H}{2}\right)^2\right\} \tag{12}$$

Furthermore, let the maximum sea-breeze velocity, at $z = -H/2$, be

$$\hat{V}_s = \hat{u}_s + i\hat{v}_s = -\frac{H^2}{8\rho_2 K_2}\left(\frac{\partial p_2}{\partial x} + i\frac{\partial p_2}{\partial y}\right) \tag{13}$$

The pressure force in the lower layer may, therefore, be expressed in terms of the maximum sea-breeze velocity, $\hat{V}_s$. Elimination of the pressure gradient from (11) and (13) gives

$$u_2 + iv_2 = \left\{1 - \left(1 + \frac{2}{H}z\right)^2\right\}(\hat{u}_s + i\hat{v}_s) + \left(1 + \frac{z}{H}\right)(u_d + iv_d) \tag{14}$$

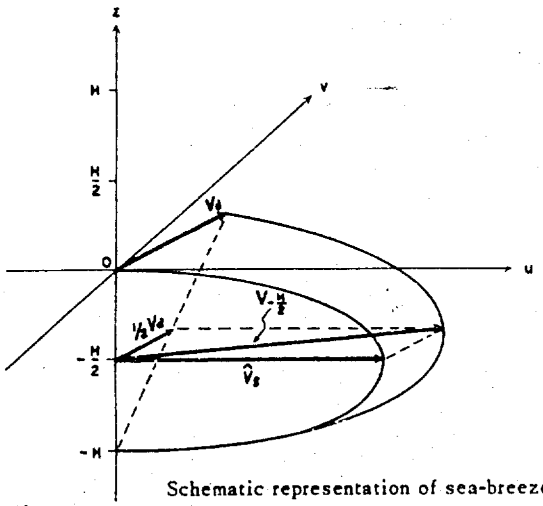

Figure 2-2 Schematic representation of sea-breeze profile and velocity of the surface of discontinuity

The velocity distribution of the fluid below the surface of discontinuity in relation to the maximum sea-breeze velocity, $\hat{V}_s$, and the velocity of the surface of discontinuity may be seen in Fig. 2-2. The quantity remaining to be determined in (10) and 14) is the velocity of the surface of discontinuity. This can be done using the condition (4). We obtain from (10) and (14) the velocity shear at the surface of discontinuity.

$$\left.\frac{\partial}{\partial z}(u_1 + iv_1)\right|_{z=o} = -(1+i)\frac{\pi}{H}\{(u_d - u_g) + i(v_d - v_g)\}$$

$$\left.\frac{\partial}{\partial z}(u_2 + iv_2)\right|_{z=o} = \frac{1}{H}\{(u_d + iv_d) - 4(\hat{u}_s + i\hat{v}_s)\} \tag{15}$$

Substitution of (15) in (4) gives

$$(u_d + iv_d) = c_o\frac{\pi}{H}\{(1+i)(u_g + iv_g) + \frac{4}{\pi}(\hat{u}_s + i\hat{v}_s) - (1 + \frac{1}{\pi} + i)(u_d + iv_d)\}$$

Solving for $(u_d + iv_d)$, we obtain

$$u_d + iv_d = \frac{\left\{(2 + \frac{H}{c_o\pi^2}) + i\frac{H}{c_o\pi^2}\right\}(u_g + iv_g) + \frac{4}{\pi}\left\{(1 + \frac{H}{c_o\pi^2}) - i\right\}(\hat{u}_s + i\hat{v}_s)}{1 + \left(1 + \frac{1}{\pi} + \frac{H}{c_o\pi}\right)^2} \tag{16}$$

It can be shown that c_o is of the order of magnitude of H/π. To estimate the velocity of the surface of discontinuity we put $c_o = H/\pi$ in (16).

$$u_d + iv_d = \frac{\{(1+2\pi) + i\}(u_g + iv_g) + 4\{(1 + \frac{1}{\pi}) - i\}(\hat{u}_s + i\hat{v}_s)}{\pi\left[1 + (2 + \frac{1}{\pi})^2\right]} \tag{17}$$

Substitution of (17) in (10) and (14) gives respectively the velocity distribution in the upper and lower layers

$$u_1 + iv_1 = \left\{1 + \frac{1}{\pi}\left[\frac{-(3 + 3\pi + \frac{1}{\pi}) + i}{1 + (2 + \frac{1}{\pi})^2}\right] e^{-(1+i)\zeta z}\right\}(u_g + iv_g)$$

$$+ \frac{4}{\pi}\left\{\frac{(1 + \frac{1}{\pi}) - i}{1 + (2 + \frac{1}{\pi})^2}\right\} e^{-(1+i)\zeta z} \quad (\hat{u}_s + i\hat{v}_s) \tag{18}$$

$$u_2 + iv_2 = \frac{1}{\pi}(1 + \frac{z}{H})\left\{\frac{(1 + 2\pi) + i}{1 + (2 + \frac{1}{\pi})^2}\right\}(u_g + iv_g)$$

$$+ \left\{1 - \left(1 + \frac{2}{H}z\right)^2 + \frac{4}{\pi}\left(1 + \frac{z}{H}\right)\left[\frac{(1 + \frac{1}{\pi}) - i}{1 + (2 + \frac{1}{\pi})^2}\right]\right\}(\hat{u}_s + i\hat{v}_s) \tag{19}$$

For a given pair of geostrophic wind and maximum sea-breeze velocities the velocity of the inversion layer may be predicted by (17), and the velocity distribution in the planetary boundary layer may be calculated from (18) and (19).

The solid curve in Fig. 2-1 is computed from (18) and (19) in which the geostrophic velocity is estimated from the wind at 2500 m whereas $\hat{u}_s + i\hat{v}_s$ is estimated by

$$(u + iv)_{z = -\frac{1}{2}H} - \frac{1}{2}(u_d + iv_d)$$

$$= 2^{-1}\left[\left(\frac{3}{2} + \frac{1}{\pi}\right) - i\right]^{-1}\left\{\pi\left[1 + \left(2 + \frac{1}{\pi}\right)^2\right](u + iv)_{z = -\frac{1}{2}H} - \frac{1}{2}\left[(1 + 2\pi) + i\right](u_g + iv_g)\right\}$$

as shown in Fig 2-3, and the wind at the middle of the lower layer is approximated by the wind at 500 m.

4. Discussion

It is seen from Fig. 2-1 that the computed hodograph gives the characteristic features of the wind distribution except in the lower part of the layer below the inversion. This deficiency may be explained as follows: (1) The topographical effect has not been taken into account; in this case the terrain near Santa Monica Airport tends to speed up the flow near the surface of the earth as indicated by the observed winds in the surface layer, however, the average wind speed over a flat plain in neighboring areas shifts its maximum to the middle of the marine layer (Edinger, 1959). (2) The replacement of an inversion layer by a surface of discontinuity in temperature exaggerates the thickness of both the lower and upper layers. The sea-breeze velocity, $\hat{V}_s$, computed from the wind at 500 m underestimates its intensity. (3) K is generally not constant with height as assumed.

It is interesting to note that however crude the model, it brings out the characteristic features of the stationary flow in the planetary boundary layer with a temperature inversion and a sea-breeze.

5. Conclusion

An analysis of the effects of an inversion layer and a sea-breeze on the stationary flow in a planetary boundary layer shows that (1) an intense temperature inversion virtually acts as a boundary surface which divides a planetary boundary layer into two layers, (2) in the lower layer the flow is primarily thermally driven whereas in the upper layer the flow is similar to that in a boundary layer of homogeneous fluid. The inversion layer moves in the direction of the resultant of the stresses acting on the layer by the fluids above and below it.

REFERENCES

Defant, F., 1949: Zur Theorie der Hangwinde, nebst Bemerkungen zur Theorie der Berg- und Talurude. Arch. Meteor. Geophys., Biokl., 1(A), 421-450.

Edinger, J. G., 1959: Wind Structure in Lowest 5 Km over Santá Monica, California. Final Report, Air Force Contract No. AF 19(604)−2424, Meteorology Department, UCLA.

Haurwitz, B., 1947: Comments on the Sea-Breeze Circulation. J. Meteor., 4, 1-8.

Neiburger, M., C. G. P. Beer, and L. B. Leopold, 1945: The California Stratus Investigation of 1944. U. S. Dept. of Comm., Weather Bureau, Washington, D.C.

Pearce, R. P., 1955: The Calculation of a Sea-Breeze Circulation in Terms of the Differential Heating across the Coast Line. Quart. Jour. Roy. Meteor. Soc., 81, 351-381.

Pierson, W. J., Jr., 1950: The Effects of Eddy Viscosity, Coriolis Deflection, and Temperaure Fluctuation on the Sea-Breeze as a Function of Time and Height. Meteor. Pap. N.Y. Univ., Vol. 1. No, 2, 29 pp.

Schmidt, F. H., 1947: An Elementary Theory of the Land- and Sea-Breeze Circulation. J. Meteor., 4, 9-15.

Smith, R. C., 1955: Theory of Air Flow over a Heated Land Mass. Quart. Jour. Roy. Meteor. Soc., 81, 382-295.

Van Bemmelen, W., 1922: Land- und Seebrise in Batavia. Beitr. Phys. frei. Atmos., 10, 169-177.

PART III

TURBULENT TRANSFER IN THE BOUNDARY LAYER OF A STRATIFIED FLUID

by S.--K. Kao

1. Introduction

In recent years, a series of wind and temperature observations under various stability ~~conditions in the surface layer has been made notably by~~ Thornthwaite and Kaser (1943), ~~and~~ by Deacon (1949). Thornthwaite and Kaser's observations brought out the characteristic features of the velocity profile in neutral and non-neutral conditions, whereas Deacon found that the observed wind profile could be represented by

$$\frac{U}{u_*} = \frac{1}{k(1-\beta)} \left\{ \left(\frac{z}{z_0}\right)^{1-\beta} - 1 \right\}$$

with

$\beta < 1$ for stable condition

$\beta = 1$ for neutral condition

$\beta > 1$ for unstable condition

where U is the mean velocity, u_* is the friction velocity, k is Von Karman's constant, z is the height, z_0 is the roughness parameter, and β is a stability parameter. Deacon's treatment has been very useful in representing data but it has its limitations. Firstly, in Deacon's formula β is assumed to be independent of height. However, Davidson and Barad (1956) found from their analysis of the micrometeorological data obtained during Project Great Plains that β decreases with height under stable conditions and increases with height under unstable conditions. Secondly, a more fundamental defect of Deacon's relation which has been pointed out by Sheppard (1958) is that it can hardly arise from a dimensionally consistent analysis of the problem.

With regard to the analytic aspect of the problem, the theory of turbulent flow in a non-neutrally stratified surface layer is notoriously difficult, although the well-known logarithmic velocity profile for a homogeneous, incompressible fluid may easily be obtained either on dimensional grounds or on the assumption of a mixing length being proportional to the distance from the surface (Prandtl, 1932). Rossby and Montgomery (1935) made the first notable analysis of the problem for a stably stratified fluid. Extensive investigations of the mechanism of the turbulent flow were made by Lettau (1949) and later by Businger (1954). Applying the similarity principle to the study of the problem Monin and Obukhov (1954) greatly simplified the analysis. However, in their treatment the function which would give the effect of the heating and cooling of the surface on turbulence has not been determined. Various related problems have not yet been settled. It is the purpose of this paper to analyze some characteristics of turbulent transfer, and determine the velocity and temperature profiles in a stratified surface layer.

2. Formulation and analysis

Consider the steady flow of a stratified fluid over an infinite uniform rough plane, with velocity variations small compared with the local velocity of sound, with temperature variations small compared with the absolute temperature, and unaffected by the rotation of the earth. Without serious loss of generality, we may suppose the mean flow to be unidirectional and horizontal, and describe the flow in a Cartesian coordinate system with the x axis in the horizontal direction of the flow and with the z axis vertically upward. In general the vertical flux of heat in the atmosphere is partly radiative. For the simplification of a theoretical analysis of the problem of transfer in surface layer we shall exclude the component of flux due to radiative transfer and consider the vertical flux of any entity to be independent of height and of the horizontal coordinate.

In conditions of neutral stability it is known that the mean velocity U at height z is given by

$$\left(\frac{dU}{dz}\right)_{\mu} = \frac{u_{*\mu}}{kz} \tag{1}$$

where the subscripts μ indicate the case of neutral stability, thus $u_{*\mu}$ is the friction velocity in neutral condition. Equation (1) implies that in neutral condition the mixing length for momentum transfer $l_{m\mu} = kz$.

Integration of (1) gives the well-known logarithmic law

$$\frac{U}{u_{*\mu}} = \frac{1}{k} \ln \frac{z}{z_o} \tag{2}$$

where the constant of integration z_o is a length characterizing the roughness of the surface. The validity of (1) and (2) for the flow of air over the land and sea has been demonstrated by Sverdrup (1936), Thornthwaite and Kaser (1943), Sheppard (1947), Pasquill (1950), Rider (1954), Hay (1955), and Deacon, Sheppard and Webb (1956).

It is obvious from (1) and (2) that in neutral condition the only parameter which needs to be considered is the friction velocity. The presence of buoyancy force and heat flux in conditions of stable and unstable stratifications suggests two parameters: gT^{-1} and $Q(\rho c_p)^{-1}$ where g is the gravity acceleration, T is the mean temperature, Q is the vertical heat flux, ρ and c_p are respectively the air density and the specific heat of the air at constant pressure. In terms of these parameters we introduce the following characteristic temperature and length

$$\Gamma = -\frac{Q}{\rho c_p u_{*\mu}}, \qquad L = \frac{u_{*\mu}^3}{k \frac{g}{T} \frac{Q}{\rho c_p}} \tag{3}$$

In a neutrally stratified surface layer the turbulence is entirely due to friction. When there is a heat flux, turbulence increases in an unstably stratified atmosphere in which convective energy is released, whereas it decreases in a stably stratified atmosphere in which convective energy is absorbed. Correspondingly, the surface stress increases in the former case and decreases in the latter. Friction velocity is therefore a function of heat flux and may be expressed by

$$u_* = u_{*\mu} \, f\left(\frac{h}{L}\right) \tag{4}$$

where h is a characteristic length and $f(hL^{-1})$ is a function to be determined having the property that as $/L/ \to \infty$ $(Q \to 0)$, u_* reduces to $u_{*\mu}$ so that $f(0) = 1$. It is to be noted that in (3) the friction velocity for neutral stability $u_{*\mu}$ is introduced instead of u_* as introduced by Monin and Obukhov (1954). This selection of parameter enables us to determine later the friction velocity in non-neutral conditions as a function of heat flux and the friction velocity in neutral stability.

Analogous to the formulation for the flux of momentum and heat in the laminar flow, let us first introduce the concept of eddy viscosity K_m and eddy conductivity K_h defined respectively by the following momentum- and heat-transfer equation

$$K_m \frac{dU}{dz} = u_*^2 \tag{5}$$

$$K_h \frac{d\theta}{dz} = -\frac{Q}{\rho c_p} \tag{6}$$

where θ is the mean potential temperature. Now, on grounds of dimensional reasoning, we generalize relationship (1) to conditions of non-neutral stratification

$$\frac{dU}{dz} = \frac{u_{*\mu}}{kz} f\left(\frac{h}{L}\right) \psi_m\left(\frac{z}{L}\right) \tag{7}$$

where ψ_m is a function of the non-dimensional variable $z\,L^{-1}$ with the property that $\psi_m \to 1$ as $/L/ \to \infty$. Substitution of (7) and (4) in (5) gives

$$K_m = kzu_{*\mu} \frac{f\left(\frac{h}{L}\right)}{\psi_m\left(\frac{z}{L}\right)} \tag{8}$$

which implies that the momentum mixing length

$$l_m = \frac{k\,z}{\psi_m\left(\frac{z}{L}\right)} \tag{9}$$

Similarly, we have for the transfer of heat

$$K_h = kzu_{*\mu} \frac{f\left(\frac{h}{L}\right)}{\psi_h\left(\frac{z}{L}\right)} \tag{10}$$

$$\frac{d\theta}{dz} = \frac{\Gamma}{kz} \frac{\psi_h\left(\frac{z}{L}\right)}{f\left(\frac{h}{L}\right)} \tag{11}$$

where $\psi_h(zL^{-1})$ is a function to be determined. Equations (10) and (11) imply that the mixing length for heat transfer

$$l_h = \frac{kz}{\psi_h\left(\frac{z}{L}\right)} \tag{12}$$

Since it has been shown experimentally (Richardson, 1920) and theoretically (Batchelor, 1953) that the Richardson number Ri can be used as a measure of the stability of the atmosphere, it is of interest to observe from (7) and (11) that

$$Ri = \frac{\frac{g}{T}\frac{d\theta}{dz}}{\left(\frac{dU}{dz}\right)^2} = \frac{-1}{\gamma f^3}\,\frac{\frac{z}{L}}{\psi_m\left(\frac{z}{L}\right)} \tag{13}$$

where $\gamma = \psi_m \psi_h^{-1} = K_h K_m^{-1}$. This indicates that the Richardson number is generally a function of height, heat flux and eddy conductivity.

3. Acceleration balance equation and generalized profiles

It has been pointed out in the previous section that atmospheric turbulence in the surface layer is caused by mechanical friction and thermal convection. Total turbulence may therefore be considered as the combination of frictional turbulence and convective turbulence. Attempts at a formulation of this relationship have been made by Rossby and Montgomery (1935), Lettau (1949) and Businger (1954). In their treatments these investigators implicitly considered frictional turbulence as an entity determined by the mean motion in condition of neutral stability. Judging from the nature of turbulent motion that the frictional turbulence and the total turbulence are generally interdependent, we shall consider the frictional turbulence to be dependent on the mean structure of the total turbulence.

We shall formulate the frictional, convective turbulence relationship in the form of acceleration. It is obvious that the total turbulence in the dimension of acceleration may be written as $l_m(dU/dz)^2$. The contribution of the frictional turbulence, which gives rise to a mixing length $l_{m\mu}$, to the acceleration of the total turbulence is $l_{m\mu}(dU/dz)^2$. The effect of buoyancy force on the motion of an eddy may be evaluated as follows: when an eddy has a temperature difference T' with its surroundings, this eddy has a convective acceleration gT'/T which on the average has a value equal to $-l_h(g/T)(d\theta/dz)$. The acceleration balance equation for turbulent flow may therefore be expressed by

$$l_m\left(\frac{dU}{dz}\right)^2 = l_{m\mu}\left(\frac{dU}{dz}\right)^2 - B\,l_h\,\frac{g}{T}\frac{d\theta}{dz} \tag{14}$$

where B is a proportionality factor as yet undetermined. A form similar to this has been studied by Elliott (1957).

Substitution of (7), (9), (11) and (13) in (14) gives

$$\psi_m^2 - \psi_m + \frac{B}{f^3}\frac{z}{L} = 0$$

Solving for ψ_m we obtain

$$\psi_m\left(\frac{z}{L}\right) = \tfrac{1}{2}\left[1 + \left(1 - \frac{4Bz}{f^3L}\right)^{1/2}\right], \text{ for } \frac{z}{f^3L} \leq \frac{1}{4B} \tag{15}$$

Here we select the solution which satisfies the property $\psi_m \to 1$ as $/L/ \to \infty$, which follows from the dimensional reasoning as analysed in the previous section. Equation (15) indicates that $\psi_m(zL^{-1})$ has two branches, one for upward heat fluxes ($Q > 0$) and the other for downward heat fluxes ($Q < 0$). In the former $0.5 \leq \psi_m \leq 1$, whereas in the latter $\psi_m \geq 1$.

By substituting (15) in (7) and by integrating z_o to z we obtain

$$\frac{U}{u_{*\mu}} = \begin{cases} \frac{f}{k}\left\{\frac{1}{2}\ln\frac{z}{z_o} + \left(1-\frac{4Bz}{f^3L}\right)^{1/2} - \left(1-\frac{4Bz_o}{f^3L}\right)^{1/2} - \tanh^{-1}\left(1-\frac{4Bz}{f^3L}\right)^{1/2} + \tanh^{-1}\left(1-\frac{4Bz_o}{f^3L}\right)^{1/2}\right\} & \text{for } Q > 0,\ \frac{z_o}{f^3L} \leq \frac{z}{f^3L} \leq \frac{1}{4B} \quad \text{(16a)} \\ \frac{1}{k}\ln\frac{z}{z_o} & \text{for } Q = 0, \quad z \geq z_o \quad \text{(16b)} \\ \frac{f}{k}\left\{\frac{1}{2}\ln\frac{z}{z_o} + \left(1-\frac{4Bz}{f^3L}\right)^{1/2} - \left(1-\frac{4Bz_o}{f^3L}\right)^{1/2} - \coth^{-1}\left(1-\frac{4Bz}{f^3L}\right)^{1/2} + \coth^{-1}\left(1-\frac{4Bz_o}{f^3L}\right)^{1/2}\right\} & \text{for } Q < 0,\ z \geq z_o \quad \text{(16c)} \end{cases}$$

Mathematically Eqs. (16a) to (16c) are valid at all heights with $U \to \infty$ as $z \to \infty$. In view of the fact that both the sources of mechanical turbulence and heat flux are located at the surface of the earth, turbulence intensity must eventually decrease with height. Eq. (16) applies only to the turbulent surface layer. Let us assume that a free stream velocity, U_s, exists at the height of the thickness of the turbulent surface layer, H_s. By substituting the free stream velocity in (16b) and (16a) or (16c) respectively for conditions of stable or unstable stratification, then by eliminating U_s from these equations, we may determine f numerically. In this case the height of the thickness of the turbulent surface layer is selected as the characteristic length h in (4). An approximate expression for f explicitly in terms of heat flux will be given in the next section.

Rider (1954) found from the analysis of his observations of wind, temperature and humidity that their profiles are rather similar over the first few meters. This implies that the eddy viscosity is proportional to eddy conductivity. If we assume that the ratio $\gamma = \psi_m \psi_h^{-1}$ = constant, Eq. (11) may be integrated,

$$\theta(z) - \theta(z_o) = \begin{cases} \frac{\Gamma}{kf\gamma}\left\{\frac{1}{2}\ln\frac{z}{z_o} + \left(1-\frac{4Bz}{f^3L}\right)^{1/2} - \left(1-\frac{4Bz_o}{f^3L}\right)^{1/2} - \tanh^{-1}\left(1-\frac{4Bz}{f^3L}\right)^{1/2} + \tanh^{-1}\left(1-\frac{4Bz_o}{f^3L}\right)^{1/2}\right\} & \text{for } Q > 0,\ \frac{z_o}{f^3L} \leq \frac{z}{f^3L} \leq \frac{1}{4B} \\ \frac{\Gamma}{kf\gamma}\left\{\frac{1}{2}\ln\frac{z}{z_o} + \left(1-\frac{4Bz}{f^3L}\right)^{1/2} - \left(1-\frac{4Bz_o}{f^3L}\right)^{1/2} - \coth^{-1}\left(1-\frac{4Bz}{f^3L}\right)^{1/2} + \coth^{-1}\left(1-\frac{4Bz_o}{f^3L}\right)^{1/2}\right\} & \text{for } Q < 0,\ z \geq z_o \end{cases} \tag{17}$$

It follows from (13) and (15) that

$$\mathrm{Ri} = \frac{-2}{\gamma} \quad \frac{-\dfrac{z}{f^3 L}}{\left\{1+\left(1-\dfrac{4Bz}{f^3 L}\right)^{1/2}\right\}} \tag{18}$$

The flux form of Richardson number (Richardson, 1920; Deacon, 1955) R_f, which is equal to the ratio of the rate at which buoyancy forces extract energy from the turbulence to the rate at which it is supplied by the shear-stress, may be expressed in the following form

$$R_f = \mathrm{Ri}\,\frac{K_h}{K_m}$$

Substitution of (18) in the above equation gives

$$R_f = \frac{-\dfrac{z}{f^3 L}}{\tfrac{1}{2}\left\{1+\left(1-\dfrac{4Bz}{f^3 L}\right)^{1/2}\right\}}$$

Richardson's arguments make it clear that R_f cannot exceed unity over any substantial depth of fluid, so it must have a maximum value (critical value) not greater than this. It is readily seen from the above equation that R_f reaches its maximum value when $4Bz(f^3L)^{-1} = 1$. The lower limiting value of the flux Richardson number is therefore

$$\underline{R}_f = -\tfrac{1}{2} \tag{18a}$$

in which B = 1 is chosen.

Townsend (1958) has recently shown that the flux Richardson number cannot exceed 0.5, which together with (18a) gives

$$-\tfrac{1}{2} \leq R_f < \tfrac{1}{2} \tag{18b}$$

The distribution of the flux Richardson number as a function of heat flux and height is shown in Fig. 3-1. It is shown in this diagram that the larger a positive heat flux the greater is the rate of decrease of the flux of Richardson number with height, whereas the smaller a negative heat flux the greater is the rate of increase of the flux of Richardson number with height.

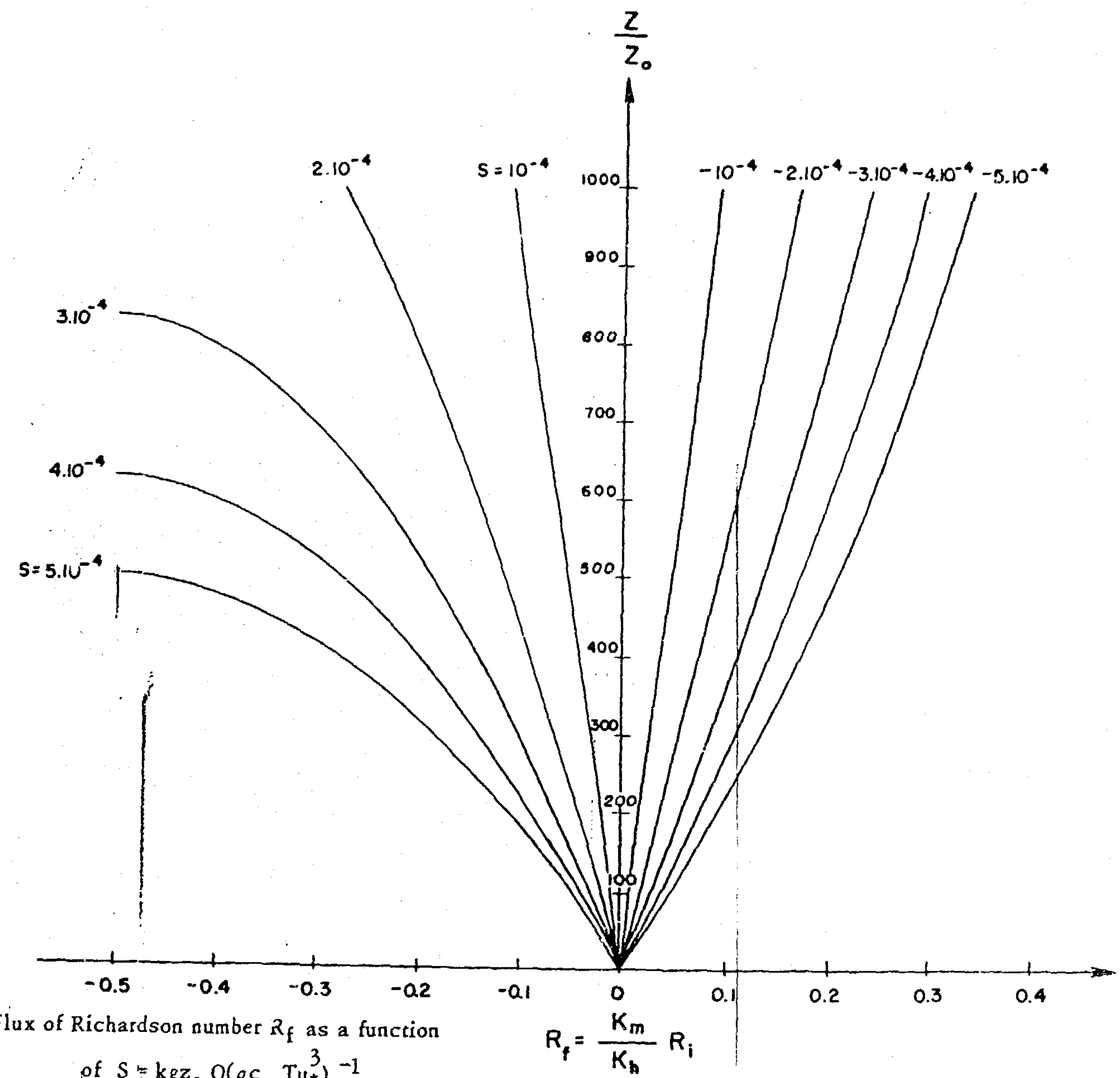

Figure 3-1 Flux of Richardson number R_f as a function of $S = kgz_o Q(\rho c_p Tu_*^3)^{-1}$.

In Fig. 3-2 the variation of non-dimensional mixing length, l_m / z_o, is exhibited for various values of non-dimensional heat flux, $S = z_o kgQ(\rho c_p T u_*^3)^{-1}$, the sloping straight line in the diagram describes the mixing length for the neutral case. The curves on the left of this line represent the mixing lengths for stable cases, the curves on the right of it represent the mixing lengths for unstable cases. The slope of mixing length decreases with height for a negative heat flux, whereas it increases with height for a positive heat flux.

4. Small values of $z(f^3 L)^{-1}$

For small values of $zf^{-3} L^{-1}$, ψ_m may be expanded in

$$\psi_m \left(\frac{z}{L}\right) = 1 - \frac{Bz}{f^3 L}, \ldots\ldots \approx 1 - \frac{Bz}{f^3 L} \quad \text{for } \frac{Bz}{f^3 L} << 1 \tag{19}$$

By substituting (19) in (7) and (11), then by integrating from z to z_o, we obtain respectively,

$$U(z) = \frac{u_{*\mu} f}{k} \left[\ln \frac{z}{z_o} - \frac{B}{f^3 L}(z - z_o)\right] \tag{20}$$

$$\theta(z) = \theta(z_o) + \frac{\Gamma}{k f \gamma}\left[\ln \frac{z}{z_o} - \frac{B}{f^3 L}(z - z_o)\right] \tag{21}$$

This gives the (logarithmic + linear)-law, the same result obtained by Monin and Obukhov (1954) through the expansion of an undetermined function with an empirical value of $B = 0.6 \pm 0.06$. Monin and Obukhov's findings are therefore the first approximation of the velocity and temperature profile (16) and (17).

To determine f, let us substitute the free stream velocity U_s, at height H_s, in (20),

$$U_s = \frac{u_{*\mu} f}{k}\left[\ln \frac{H_s}{z_o} - \frac{B}{f^3 L}(H_s - z_o)\right] \tag{22}$$

which becomes for neutral stability ($/L/ \to \infty$ and $f = 1$),

$$U_s = \frac{u_{*\mu}}{k} \ln \frac{H_s}{z_o} \tag{23}$$

Here we assume that the free stream velocity is unaffected by the heat flux in the surface boundary layer. Elimination of Us from (22) and (23) results in

$$f^3 - f^2 - \frac{B(H_s - z_o)}{L \ln (H_s/z_o)} = 0 \tag{24}$$

Although it can readily be shown that the real solution of (24) is

$$f = \frac{1}{3} + \frac{1}{3}\left\{1 + \frac{27}{2}\xi\left[1 + \left(1 + \frac{4}{27\xi}\right)^{1/2}\right]\right\}^{\frac{1}{3}} + \frac{1}{3}\left\{1 + \frac{27}{2}\xi\left[1 - \left(1 + \frac{4}{27\xi}\right)^{1/2}\right]\right\}^{\frac{1}{3}} \tag{25}$$

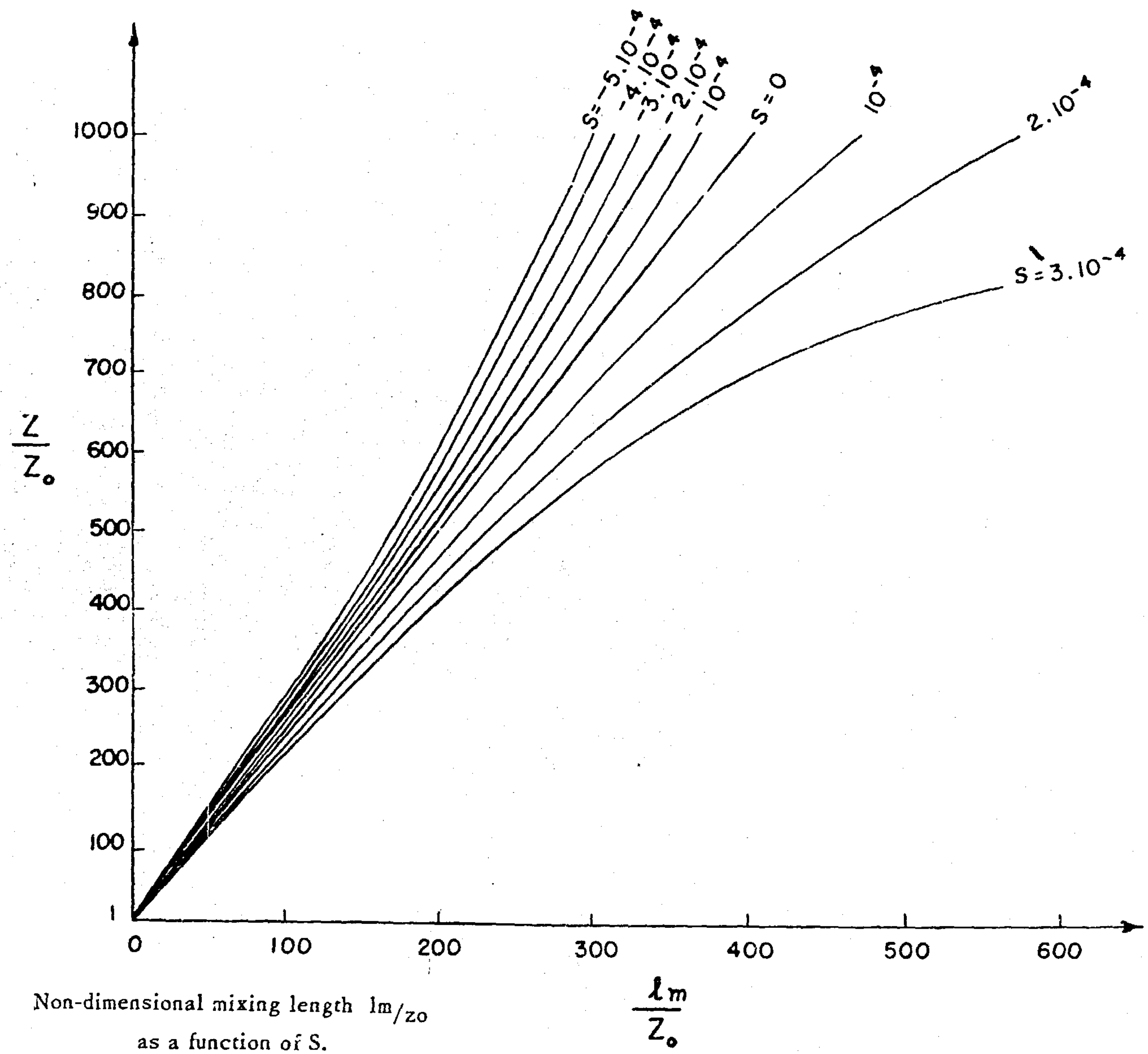

Figure 3-2 Non-dimensional mixing length l_m/z_o as a function of S.

where $\xi = B(H_s - z_o)\ [L\ln(H_s/z_o)]^{-1}$, an expression for f simpler than (25) may be obtained. This will simplify the computation. A careful examination of (16) indicates that at a certain height between z_o and H_s the velocity shear in non-neutral stratification is equal to that in neutral stability. Let this height be h_o; we have by definition

$$\left.\frac{dU}{dz}\right|_{z=ho} = \left.\left(\frac{dU}{dz}\right)_\mu\right|_{z=ho} \tag{26a}$$

Substitution of (1) and (7) in the above equation with the use of (15) gives

$$f^2 - f - \frac{Bho}{L} = 0 \tag{26b}$$

Solving for f we obtain

$$f = \tfrac{1}{2}\left[1 + \left(1 + \frac{4Bho}{L}\right)^{1/2}\right] \tag{27}$$

Here we select the solution which satisfies the condition that $f = 1$ as $/L/\to\infty$.

It can be shown by substituting (1) and (7) in (26a) with the use of (19) that

$$f^3 - f^2 - \frac{Bho}{L} = 0$$

Comparison of the above equation with (24) gives the value of h_o

$$ho = \frac{H_s - Z_o}{\ln \dfrac{H_s}{Z_o}} \tag{28}$$

By substituting (28) in (27) we obtain

$$f = \tfrac{1}{2}\left[1 + \left(1 + \frac{4B(H_s - z_o)}{L\ln(H_s/z_o)}\right)^{1/2}\right] \approx 1 + \frac{B(H_s - z_o)}{L\ln(H_s/z_o)} \tag{29}$$

It follows from (4) that

$$u_* = u_{*\mu}\left[1 + \frac{B(H_s - z_o)}{L\ln(H_s/z_o)}\right] \tag{30}$$

This indicates that an upward heat flux ($Q > 0$) increases the friction velocity, whereas a downward heat flux ($Q < 0$) decreases the friction velocity. This agrees with what we have anticipated from the energy consideration in section 2.

Although for small values of $z\,L^{-1}$ velocity profiles may be estimated by (22), a more precise distribution of non-dimensional velocity $U/u_{*\mu}$ (16) is shown in Fig. 3-3 in which $H_s/z_o = 3.10^3$ is chosen. The sloping straight line in the diagram describes the logarithmic profile for the neutral case. The curves on the left of this line represent the velocity profiles for stable cases; the curves on the right of it represent the velocity profiles for unstable cases. At the roughness height the velocity shear in stable conditions is smaller than that in the

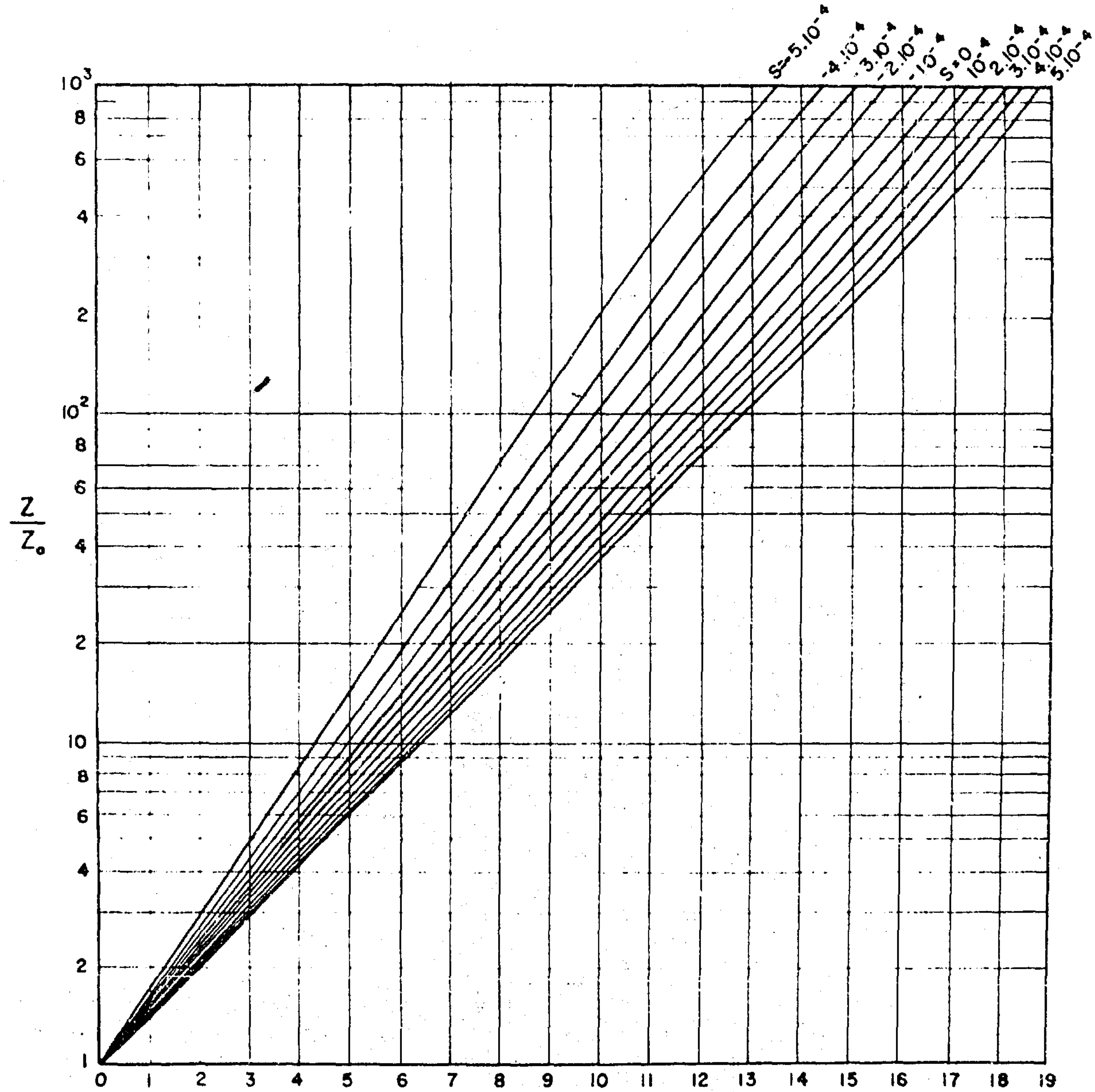

Figure 3-3 Non-dimensional velocity $U/u_{*\mu}$ as a function of S.

neutral condition, whereas the latter is smaller than that in unstable conditions. A characteristic feature of these profiles is that the velocity profiles for the non-neutral cases converge toward the profile for the neutral case in the higher level. This agrees with the classical profiles observed by Thornthwaite and Kaser (1943).

It is of practical interest to determine the velocity profile and heat flux from wind observations alone. For example, if we have wind observations at three levels, z_1, z_2 and z_3, we can determine the velocity profile and heat flux as follows: with the use of (20) it can be shown that

$$u_* = k \frac{(U_2 - U_1)(z_3 - z_2) - (U_3 - U_2)(z_2 - z_1)}{(z_3 - z_2)\ln(z_2/z_1) - (z_2 - z_1)\ln(z_3/z_2)} \tag{31}$$

$$f^3 L = B \frac{(U_2 - U_1)(z_3 - z_2) - (U_3 - U_2)(z_2 - z_1)}{(U_2 - U_1)\ln(z_3/z_2) - (U_3 - U_2)\ln(z_2/z_1)} \tag{32}$$

By substituting (31) and (32) in (20) we can determine the wind profile in the turbulent surface layer. The heat flux can be determined from (31), (32) and (3),

$$Q = \frac{\rho c_p k^2 T}{gB} \frac{[(U_2-U_1)\ln(z_3/z_2) - (U_3-U_2)\ln(z_2/z_1)][(U_2-U_1)(z_3-z_2) - (U_3-U_2)(z_2-z_1)]^2}{[(z_3-z_2)\ln(z_2/z_1) - (z_2-z_1)\ln(z_3/z_2)]^3} \tag{33}$$

If both wind and temperature observations are available, velocity and temperature profiles may be determined from observations at two levels. It can be shown with the use of (20) and (21) that

$$u_* = k \frac{(U_2 - U_1)^2 - B\frac{g}{T}(\theta_1 - \theta_2)(z_2 - z_1)}{(U_2 - U_1)\ln(z_2/z_1)} \tag{34}$$

$$Q = \rho c_p u_*^2 \frac{\theta_1 - \theta_2}{U_2 - U_1} \tag{35}$$

Here $\gamma = 1$ is assumed. By substituting (29) in (34) the friction velocity for neutral condition, $u_{*\mu}$, may be determined.

5. Conclusion

An analysis is made of some characteristics of the steady turbulent transfer in the boundary layer of a stratified fluid. The effects of the heat flux on the variation of the mixing length and the flux of Richardson number are determined. The velocity and temperature profiles are derived. It is found that velocity profiles for non-neutral cases converge in the higher level towards the profile for the neutral condition, a characteristic which agrees with velocity profile observed by Thornthwaite and Kaser (1943). It is shown that Monin and Obukhov's findings become the first approximation of equations (16a) and (16c). For a constant free stream velocity an upward heat flux increases the friction velocity, whereas a downward heat flux decreases the friction velocity. The lower limiting value of the flux Richardson number is found to be -0.5, which, together with the upper limiting value, 0.5, obtained by Townsend (1958), gives the range of the flux Richardson number.

REFERENCES

Batchelor, G. K., 1953: The condition for dynamical similarity of motions of a frictionless perfect-gas atmosphere. Quart. J. r. Meteor. Soc., 79, 224-235.

Businger, J.A., 1954: Some aspects of the influence of the earth's surface on the atmosphere. Meded. Verh. k. Ned. Meteor. Inst., No. 61, 78 pp.

Davidson, B., and M. L. Barad, 1956: Some comments on the Deacon wind profile. Trans., American Geophys. Union, 37, No. 2, 168-176.

Deacon, E. L., 1949: Vertical diffusion in the lowest layer of the atmosphere. Quart. J. r. Meteor. Soc., 75, 89-103.

———, 1955: Turbulent transfer of momentum in the lowest layers of the atmosphere. Div. Met. Phys. Tech. Paper No. 4, C.S.I.R.D., Melbourne.

———, P. A. Sheppard and E. K. Webb, 1956: Wind profiles over the sea and the drag at the sea surface. Austrian J. Phys., 9, 511-541.

Elliott, W. P., 1957: A comparison of some approaches to the diabatic wind profile. Trans., American Geophys. Union, 38, No. 1, 21-24.

Hay, J. S., 1955: Some observations of air flow over the sea. Quart. J. r. Meteor. Soc., 81, 307-319.

Lettau, H., 1949: Isotropic and non-isotropic turbulence in the atmospheric surface layer. Geophys. Res. Paper, No. 1, Air Force Cambridge Res. Directorate, 84 pp.

Monin, A. S. and A. M. Obukhov, 1954: Fundamental law of turbulent exchange in the surface layer. Works of Geophys. Inst., 151, No. 24, 163-186.

Pasquill, L., 1949: Eddy diffusion of water vapor and heat near the ground. Proc. roy. Soc., London, A, 198, 116-140.

Prandtl, L., 1932: Meteorologische Anwendung der Strömungslehre. Beitr. Physik. fr. Atmos., 19, 188-202.

Richardson, L. F., 1920: The supply of energy from and to atmospheric eddies. Proc. roy. Soc., London, A, 97, 354-373.

Rider, N. E., 1954: Eddy diffusion of momentum, water vapor and heat near the ground. Phil. Trans. roy. Soc., London, A, 246, 481-501.

Rossby, C. -G. and R. B. Montgomery, 1935: The layer of frictional influence in wind and ocean currents. Pap. Phys., Ocean. Meteor., Mass. Inst. Tech. and Woods Hole Ocean. Inst., 3, No. 3, 101 pp.

Sheppard, P. A., 1947: The aerodynamic drag of the earth's surface and the value of Von Karman's constant in the lower layer. Proc. roy. Soc., London, A, 188, 208-222.

———, 1958: Transfer across the earth's surface and through the air above. Quart. J. roy. Meteor. Soc., 84, 205-224.

REFERENCES (cont.)

Sverdrup, H. V., 1936: The eddy conductivity of the air over a smooth snow field. Geophys. Pub., 11, No. 7.

Thornthwaite, C. W. and P. Kaser, 1943: Wind-gradient observations. Trans., American Geophys. Union, 24, 166-182.

Townsend, A. A., 1958: Turbulent flow in a steady stratified atmosphere. J. Fluid Mechanics, 3, 361-372.